

Shadow and gravitational weak lensing around a quantum-corrected black hole surrounded by plasma*

Mirzabek Alloqulov^{1,2}[✉][✉] Yokubjon Isaqjonov¹[✉] Sanjar Shaymatov^{1,3,4,5}[✉][✉] Abdul Jawad^{6,7}[✉][✉]

¹University of Tashkent for Applied Sciences, Str. Gavhar 1, Tashkent 100149, Uzbekistan

²Shahrisabz State Pedagogical Institute, Shahrisabz Str. 10, Shahrisabz 181301, Uzbekistan

³Tashkent State Technical University, Tashkent 100095, Uzbekistan

⁴Samarkand State University, University Avenue 15, 140104 Samarkand, Uzbekistan

⁵Western Caspian University, Baku AZ1001, Azerbaijan

⁶Institute for Theoretical Physics and Cosmology, Zhejiang University of Technology, Hangzhou 310023, China

⁷Department of Mathematics, COMSATS University Islamabad, Lahore Campus, Lahore-54000, Pakistan

Abstract: In this study, we investigate the optical properties of a quantum-corrected black hole (BH) in loop quantum gravity surrounded by a plasma medium. First, we determine the photon and shadow radii resulting from quantum corrections and the plasma medium in the environment surrounding a quantum-corrected BH. Our findings indicate that the photon sphere and BH shadow radii decrease owing to the quantum correction parameter α , which acts as a repulsive gravitational charge. Further, we investigate the gravitational weak lensing by applying the general formalism used to model the deflection angle of the light traveling around the quantum-corrected BH within the plasma medium. We show, in conjunction with the fact that the combined effects of the quantum correction and non-uniform plasma frequency parameter can decrease the deflection angle, that the light traveling through the uniform plasma can be strongly deflected than the non-uniform plasma environment surrounding the quantum-corrected BH. Finally, we examine the magnification of the lensed image brightness under the effect of the quantum correction parameter α , including the uniform and non-uniform plasma effects.

Keywords: quantum-corrected black hole, gravitational weak lensing, photon motion, shadow

DOI: 10.1088/1674-1137/ad9f44 **CSTR:** 32044.14.ChinesePhysicsC.49045104

I. INTRODUCTION

In general relativity (GR), astrophysical black holes (BHs) form from the collapse of a self-gravitating massive star at the end-state evolution, thereby making GR the most successful theory of gravity. However, there exist theoretical challenges that must be addressed, such as quantization, dark matter and energy issues, singularities inside BHs [1] and at the beginning of the universe [2, 3], where GR breaks down. Additionally, GR does not incorporate quantum principles, thereby leaving the unification of GR and quantum mechanics unsolved [4, 5]. These challenges have been explored from various perspectives, with modified and quantum theories of gravity proposed as potential solutions. Testing these modified theories of gravity in astrophysical scenarios is crucial for developing a final theory that can address the limitations

of GR. Despite these challenges, recent observations such as gravitational waves (GWs) [6, 7] and the BH shadow [8, 9]) offer promising insights into the GR issues.

As previously stated, GR is unable to incorporate quantum principles or find a solution to cosmological Big Bang and BH singularities. Consequently, quantum theories of gravity may offer a potential solution to address these singularities through quantum effects. In this regard, loop quantum gravity (LQG) has emerged as a non-perturbative theory of quantum gravity [10]. Since then, its techniques have been extensively applied to addressing these singularities in loop quantum cosmology; see Refs. [11–17]. Models that describe BH solutions in LQG have been developed in recent years. For example, a regular static BH solution, known as the self-dual BH, was obtained within a mini-superspace framework using the polymerization procedure in LQG [18], thereby exhibit-

Received 1 October 2024; Accepted 13 December 2024; Published online 14 December 2024

* Supported by the National Natural Science Foundation of China (11675143) and the National Key Research and Development Program of China (2020YFC2201503)

[✉] E-mail: malloqulov@gmail.com

[✉] E-mail: isaqjonovoqubjon@gmail.com

[✉] E-mail: sanjar@astrin.uz

[✉] E-mail: jawadab181@yahoo.com

©2025 Chinese Physical Society and the Institute of High Energy Physics of the Chinese Academy of Sciences and the Institute of Modern Physics of the Chinese Academy of Sciences and IOP Publishing Ltd. All rights, including for text and data mining, AI training, and similar technologies, are reserved.

ing self-duality associated with T-duality principles [19, 20]. Extensive analyses have provided insights into the nature of quantum BH solutions, with focus on examining the quantum effects within the LQG framework; see Refs. [21–29]. Additionally, recent years have witnessed a growing interest in the phenomenological study of loop quantum black holes, which has been extensively explored across various contexts; see Refs. [30–37].

The detection of the first image of BHs [8, 9] has opened up new avenues to develop theoretical models that can test various theories of gravity by exploring BH shadows. For a BH shadow, light can follow geodesics and orbit the BH, thereby leading to a dark disk. This analysis was first conducted for the Schwarzschild BH [38], including its image [39]. The BH shadow is envisioned as a dark region surrounded by a light ring in the sky, with a dark disk formed by light trapped within the gravitational pull of the BH. Investigating BH accretion disks is crucial for understanding its characteristics and spacetime geometry. Further, the BH shadow was explored by Amarilla *et al.* for a rotating Kaluza-Klein dilaton BH [40] and extended to the Einstein-Maxwell-Dilaton-Axion BH [41]. In recent years, there has been an increase in activity, with the BH shadow being investigated based on different perspectives [42–51]. The BH shadow was investigated for a rotating BH including a scalar dilaton field [52], a charged BH with a dilaton field within the Einstein-Maxwell-scalar theory [53], and regular BHs [54]. It was demonstrated that the BH deformation parameters can significantly affect the BH shadow characteristics (see [55]), while recent EHT observations can be used to restrict theoretical BH shadow models [56]. Additionally, the modified theory of gravity (MOG) was tested using the BH shadow analysis in both rotating and non-rotating cases [57–59].

In an astrophysical scenario, BHs can be surrounded by a plasma medium in their nearby environment, wherein the optical properties of the BHs, such as the shadow and gravitational lensing effects, can be significantly altered owing to the surrounding plasma effect. Gravitational lensing effects occur owing to the highly deflected light traveling around a BH in the strong field regime, thereby leading to the first theoretical experiment wherein GR was successfully tested using gravitational lensing analysis (see [60]). Gravitational lensing effects can also provide excellent tests for probing spacetime geometry, particularly in regions very close to the BH horizon. Therefore, in recent years, there has been increased research activity addressing gravitational lensing effects in the weak form (see, *e.g.*, [61–72]) in the presence of a plasma medium (see [73–80]) within various gravity scenarios.

BHs are the most fascinating and intriguing astrophysical objects, and are currently being investigated based on different theoretical and observational perspect-

ives. This analysis provides valuable insights into BH properties across different models, such as a quantum-corrected BH solution, which incorporates quantum corrections within the Oppenheimer-Snyder model in the context of loop quantum gravity [80]. In this solution, the BH mass is subjected to a lower bound owing to quantum corrections, thereby leading to a different background geometry than the BH solutions in GR. This quantum-corrected BH solution was developed as a modification of the Schwarzschild BH, thereby addressing the BH singularity. Notably, its geometry may differ from other BH solutions derived within loop quantum gravity, thereby showing that the collapsing process depends on whether the collapsing matter density extends to the Planck scale. If this density is of the order of the Planck scale, the collapsing process transforms into a bounce expansion epoch. Based on [80], numerous studies [81–85] have investigated the properties of this quantum-corrected BH spacetime under various situations. Therefore, it is crucial to investigate the optical properties of a quantum-corrected BH to understand the potential deviations from GR resulting from quantum corrections within loop quantum gravity. In this study, we explore the optical properties of a quantum-corrected BH, including the BH shadow and gravitational lensing effects amidst a plasma medium. This analysis enhances our understanding of the unique features of quantum-corrected BH geometry.

This paper is organized as follows: In Sec. II, we briefly review a quantum-corrected BH spacetime and discuss the formalism used to model the photon motion and BH shadow in a plasma medium. In Sec. III, we investigate the gravitational lensing effects around a quantum-corrected BH, including the plasma medium effects resulting from both uniform and non-uniform cases. In Sec. IV, we analyze a magnification of gravitationally lensed images around a quantum-corrected BH. Finally, we conclude in Sec. V. For simplicity, we shall use $c = G = M = 1$ throughout the paper.

II. SPACETIME METRIC AND NULL GEODESICS

Here, we briefly review the dynamics of the photon motion to explore the BH shadow under the combined effects of the plasma medium and quantum corrections resulting from the loop quantum gravity. The corresponding metric describing a static and spherically symmetric quantum-corrected BH in Boyer-Lindquist coordinates (t, r, θ, ϕ) is expressed as follows [80]:

$$ds^2 = -f(r)dt^2 + f(r)^{-1}dr^2 + r^2d\Omega^2, \quad (1)$$

with

$$f(r) = \left(1 - \frac{2GM}{r} + \frac{\alpha G^2 M^2}{r^4}\right), \quad (2)$$

where M represents the Arnowitt–Deser–Misner mass and $\alpha = 16\sqrt{3}\pi\gamma^3\ell_p^2$ the quantum corrected parameter, including the Immirzi parameter γ and Planck length $\ell_p = \sqrt{G\hbar}$. For simplicity, we will assume α as a dimensionless quantity by considering $\alpha \rightarrow \alpha/M^2$ and setting $G = c = 1$. The metric describing the quantum-corrected BH as expressed in Eq. (1) can be reduced to the Schwarzschild BH in the limit where $\alpha \rightarrow 0$.

Photon motion around the quantum-corrected BH immersed in the plasma medium: Here, we consider the formalism used to model and investigate the motion of the photon around the quantum-corrected BH based on the Hamilton-Jacobi equation. First, we write the Hamiltonian for null geodesics around the BH amidst the plasma medium, which is expressed as follows [86]:

$$\mathcal{H}(x^\alpha, p_\alpha) = \frac{1}{2} [g^{\alpha\beta} p_\alpha p_\beta - (n^2 - 1)(p_\beta u^\beta)^2], \quad (3)$$

where x^α represents the spacetime coordinates, u^β and p_α the four-velocity and momentum of the photon, respectively, and n the refractive index, *i.e.*, $n = \omega/k$, where k is the wave number. The equation for the refractive index can be written as follows [87]:

$$n^2 = 1 - \frac{\omega_p^2}{\omega^2}, \quad (4)$$

where $\omega_p^2(x^\alpha) = 4\pi e^2 N(x^\alpha)/m_e$ represents the plasma frequency, with m_e and e denoting the electron mass and charge, respectively. N represents the number density of the electrons. Using the expression $\omega^2 = (p_\beta u^\beta)^2$, the photon frequency is expressed as follows:

$$\omega(r) = \frac{\omega_0}{\sqrt{f(r)}}, \quad \omega_0 = \text{const.} \quad (5)$$

If r tends to infinity ($r \rightarrow \infty$), the lapse function $f(r)$ tends to 1. Hence, $\omega(\infty) = \omega_0 = -p_t$ expresses the photon energy at spatial infinity [88]. ω_0 can be restricted using the photon geodesics $\mathcal{H} = 0$ as expressed as follows:

$$\frac{\omega_0^2}{f(r)} > \omega_p^2(r). \quad (6)$$

From a physical viewpoint, the restriction means that photon frequency at a given point ($\omega(r)$) must be greater than the plasma frequency at a similar point. This rule can be consistently applied to light propagation in a plasma. Hence, the BH shadow can have different forms from the vacuum case $\omega_p = 0$. Using the Eq. (4), we can rewrite Eq. (3) for the light geodesics amidst a plasma medium as follows:

$$\mathcal{H} = \frac{1}{2} [g^{\alpha\beta} p_\alpha p_\beta + \omega_p^2]. \quad (7)$$

The four velocities for the photon in the equatorial plane ($\theta = \pi/2$) can be expressed as follows:

$$t \equiv \frac{dt}{d\lambda} = \frac{-p_t}{f(r)}, \quad (8)$$

$$\dot{r} \equiv \frac{dr}{d\lambda} = p_r f(r), \quad (9)$$

$$\dot{\phi} \equiv \frac{d\phi}{d\lambda} = \frac{p_\phi}{r^2}, \quad (10)$$

where $\dot{x}^\alpha = \partial\mathcal{H}/\partial p_\alpha$. The orbit equation is obtained using Eqs. (9) and (10) as follows:

$$\frac{dr}{d\phi} = \frac{g^{rr} p_r}{g^{\phi\phi} p_\phi}. \quad (11)$$

The above equation for the photon geodesics can be rewritten as follows: $\mathcal{H} = 0$

$$\frac{dr}{d\phi} = \sqrt{\frac{g^{rr}}{g^{\phi\phi}}} \sqrt{\gamma^2(r) \frac{\omega_0^2}{p_\phi^2} - 1}, \quad (12)$$

where the following relation holds as follows:

$$\gamma^2(r) \equiv -\frac{g^{tt}}{g^{\phi\phi}} - \frac{\omega_p^2}{g^{\phi\phi} \omega_0^2}. \quad (13)$$

A light ray originates from infinity, reaches a minimum at a radius r_{ps} , and then returns to infinity. Mathematically, this corresponds with a turning point of the $\gamma^2(r)$ function. Hence, the radius of the photon sphere can be expressed using the following equation:

$$\left. \frac{d(\gamma^2(r))}{dr} \right|_{r=r_{ps}} = 0. \quad (14)$$

Solving the above equation is challenging. Hence, we use the numerical method and plot the dependence of the photon radius on the BH and plasma parameters shown in Fig. 1. As shown in Fig. 1, the value of the photon radius increases with an increase in the plasma parameter. Further, the photon radius decreases as the quantum corrected parameter α increases. This corresponds with the interpretation of the quantum-corrected parameter as a repulsive gravitational charge, which physically manifests in a change of the causal structure, thereby weakening the

gravitational field strength at close distances near the quantum-corrected BH. This allows for photon orbits to remain closer to the BH.

The quantum-corrected black hole shadow in the plasma medium: Here, we investigate the BH shadow radius in the presence of the plasma medium. To provide more information, we demonstrate the trajectory of the photon as shown in Fig 2. Herein, the angle α approaches α_{sh} , while the radius of the shadow R tends to r_{ps} . Further, we can explore the BH shadow using this figure. The angular radius α_{sh} of the BH can be expressed as follows [42, 88]:

$$\sin^2 \alpha_{\text{sh}} = \frac{\gamma^2(r_{\text{ps}})}{\gamma^2(r_o)}, = \frac{r_{\text{ps}}^2 \left[\frac{1}{f(r_{\text{ps}})} - \frac{\omega_p^2(r_{\text{ps}})}{\omega_0^2} \right]}{r_o^2 \left[\frac{1}{f(r_o)} - \frac{\omega_p^2(r_o)}{\omega_0^2} \right]}, \quad (15)$$

where r_{ps} and r_o represent the locations of the photon sphere and observer, respectively. We can approximate the radius of the BH shadow for the observer located at a sufficiently large distance from the BH as expressed as follows [88]:

$$R_{\text{sh}} \simeq r_o \sin \alpha_{\text{sh}}, = \sqrt{r_{\text{ps}}^2 \left[\frac{1}{f(r_{\text{ps}})} - \frac{\omega_p^2(r_{\text{ps}})}{\omega_0^2} \right]}. \quad (16)$$

We demonstrate the dependence of the BH shadow on the plasma and BH parameter as shown in Fig. 3. Herein, the radius of the BH shadow decreased with an increase in the plasma parameter. Under the influence of the α parameter, the radius of the BH shadow decreased slightly. We assume that the compact objects Sgr A* and M87* are static and spherically symmetric, even though the observations from the EHT collaboration do not support this assumption. Further, we try to theoretically ex-

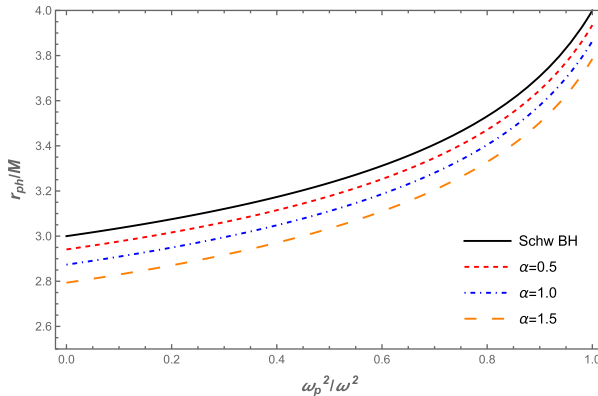


Fig. 1. (color online) Left panel: The radius of the photon sphere as a function of the plasma frequency for different values of the α parameter. Right panel: The dependence of the radius of the photon sphere on the α parameter for different values of the plasma frequency.

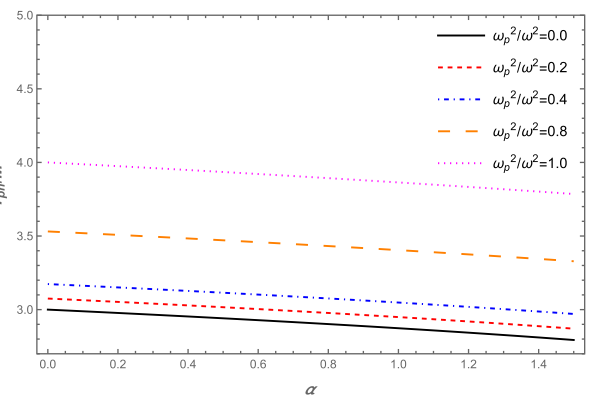
plore the lower limits of the α parameter using the data provided by the EHT collaboration project. We chose the α parameter and plasma frequency for constraint. We can constrain both quantities, α and ω_p^2/ω^2 , using the observational data provided by the EHT collaboration regarding the shadows of the supermassive BHs Sgr A* and M87*. The angular diameter $\theta_{\text{M87}*}$ of the BH shadow, the distance from Earth and mass of the BH at the center of the M87* are $\theta_{\text{M87}*} = 42 \pm 3 \mu\text{as}$, $D = 16.8 \pm 0.8 \text{ Mpc}$, and $M_{\text{M87}*} = 6.5 \pm 0.7 \times 10^9 M_\odot$ [8], respectively. For Sgr A*, the data provided by the EHT collaboration are $\theta_{\text{SgrA}*} = 48.7 \pm 7 \mu\text{as}$, $D = 8277 \pm 9 \pm 33 \text{ pc}$ and $M_{\text{SgrA}*} = 4.297 \pm 0.013 \times 10^6 M_\odot$ (VLTI) [89]. Using this information, the diameter of the shadow caused by the compact object per unit mass can be expressed as follows [90]:

$$d_{\text{sh}} = \frac{D\theta}{M}. \quad (17)$$

Using the expression $d_{\text{sh}} = 2R_{\text{sh}}$, one can easily obtain the expression for the BH shadow diameter. The distance D is considered a dimension of M [8, 9]. The resulting values for the diameter of the BH shadow are applicable to $d_{\text{sh}}^{\text{M87}*} = (11 \pm 1.5)M$ for M87* and $d_{\text{sh}}^{\text{SgrA}*} = (9.5 \pm 1.4)M$ for Sgr A*. The lower limits of the quantities α and ω_p^2/ω^2 for the supermassive BHs at the centers of the galaxies Sgr A* and M87* can be found using the observational EHT data, as shown in Fig. 4.

III. WEAK GRAVITATIONAL LENSING FOR BLACK HOLE

In this section, we explore the weak gravitational lensing under two different plasma distributions: uniform and non-uniform plasma. To begin, we express the weak-field approximation as [64, 91]



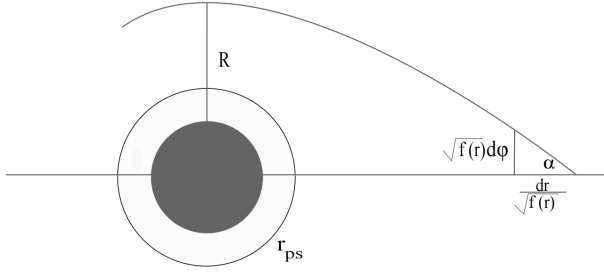


Fig. 2. Schematic of the light bending around the BH. As R approaches r_{ps} , the angle α converges to the angular radius of the BH shadow α_{sh} .

$$g_{\alpha\beta} = \eta_{\alpha\beta} + h_{\alpha\beta}, \quad (18)$$

where $\eta_{\alpha\beta}$ and $h_{\alpha\beta}$ represents the expressions for the Minkowski spacetime and perturbation gravity field, respectively. The following conditions can be rewritten for them:

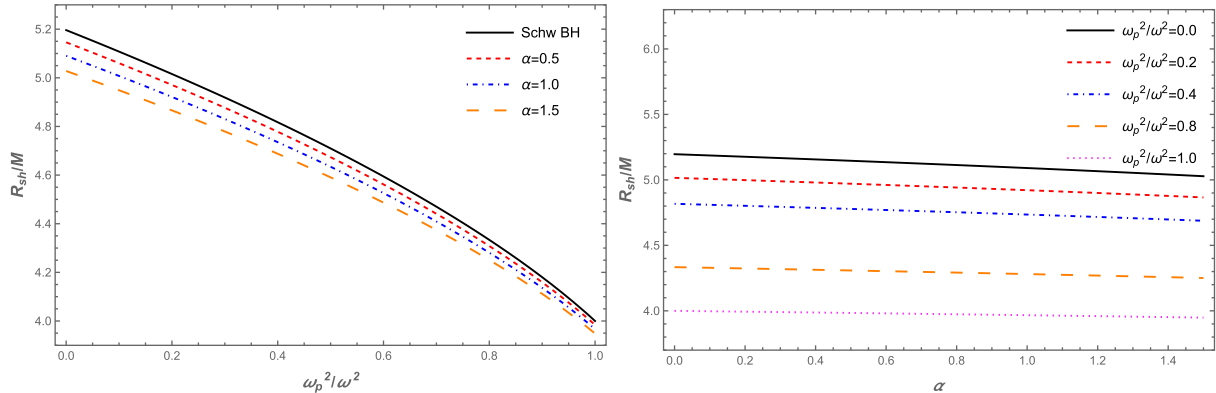


Fig. 3. (color online) Left panel: The radius of the BH shadow as a function of the plasma frequency for different values of the α parameter. Right panel: The dependence of the radius of the BH shadow on the α parameter for different values of the plasma frequency.

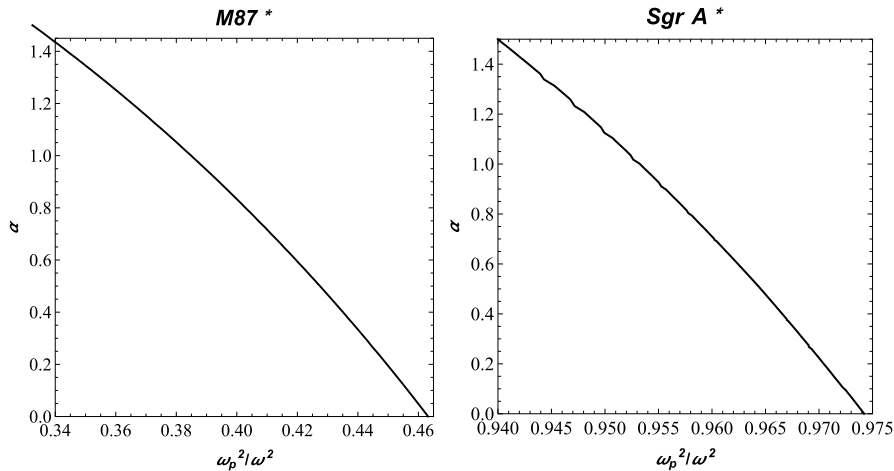


Fig. 4. Constrained values of the α parameter and ω_p^2/ω_0^2 for the supermassive BHs at the centers of the M87 and Sgr A* galaxies.

with $ds_0^2 = -dt^2 + dr^2 + r^2(d\theta^2 + \sin^2\theta d\phi^2)$. Later, we can define the components of $h_{\alpha\beta}$ as the perturbations which are expressed as follows:

$$h_{00} = \frac{2M}{r} - \frac{\alpha M^2}{r^4}, \quad (22)$$

$$h_{ik} = \left(\frac{2M}{r} - \frac{\alpha M^2}{r^4} \right) n_i n_k, \quad (23)$$

$$h_{33} = \left(\frac{2M}{r} - \frac{\alpha M^2}{r^4} \right) \cos^2\chi, \quad (24)$$

with $\cos^2\chi = z^2/(b^2 + z^2)$ and $r^2 = b^2 + z^2$. The first derivatives of h_{00} and h_{33} with respect to the radial coordinate can be expressed as follows:

$$\frac{dh_{00}}{dr} = -\frac{2M}{r^2} + \frac{4\alpha M^2}{r^5}, \quad (25)$$

$$\frac{dh_{33}}{dr} = -\frac{2Mz^2}{r^4} + \frac{4\alpha M^2 z^2}{r^7}. \quad (26)$$

The deflection angle can be expressed as follows:

$$\hat{\alpha}_b = \hat{\alpha}_1 + \hat{\alpha}_2 + \hat{\alpha}_3, \quad (27)$$

with

$$\begin{aligned} \hat{\alpha}_1 &= \frac{1}{2} \int_{-\infty}^{\infty} \frac{b}{r} \frac{dh_{33}}{dr} dz, \\ \hat{\alpha}_2 &= \frac{1}{2} \int_{-\infty}^{\infty} \frac{b}{r} \frac{1}{1 - \omega_p^2/\omega^2} \frac{dh_{00}}{dr} dz, \\ \hat{\alpha}_3 &= \frac{1}{2} \int_{-\infty}^{\infty} \frac{b}{r} \left(-\frac{K_e}{\omega^2 - \omega_p^2} \frac{dN}{dr} \right) dz. \end{aligned} \quad (28)$$

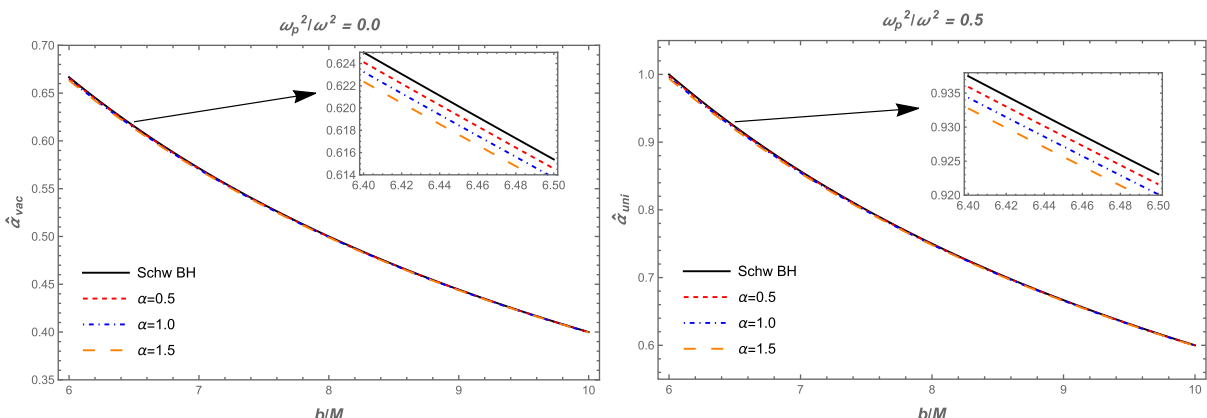


Fig. 5. (color online) Left panel: The dependence of the deflection angle $\hat{\alpha}_{vac}$ on the impact parameter b for the different values of the α parameter. Here, $\omega_p^2/\omega^2 = 0$. Right panel: The dependence of the deflection angle $\hat{\alpha}_{uni}$ on the impact parameter b for the different values of the parameter α .

In the aforementioned, we explore the impact of plasma density distributions on the deflection angle from two different perspectives: uniform and non-uniform plasma cases.

Uniform plasma distribution: Here, we consider a uniform plasma surrounding the quantum-corrected BH and examine its impact on the gravitational angle of deflection. Hence, we rewrite Eq. (27) to account for the uniform plasma as follows:

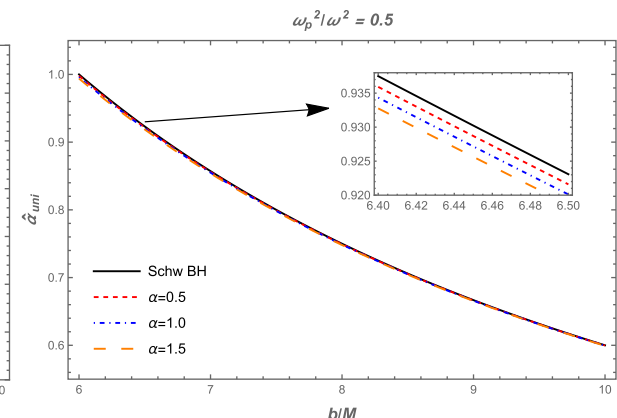
$$\hat{\alpha}_{uni} = \hat{\alpha}_{uni1} + \hat{\alpha}_{uni2} + \hat{\alpha}_{uni3}. \quad (29)$$

The deflection angle influenced by a uniform plasma can be expressed using Eqs. (24), (27) and (28). The dependence of the deflection angle on the impact parameter b is shown in Fig. 5. The left panel represents the vacuum case, where there is a slight decrease in the deflection angle as the α parameter increases. The right panel shows the uniform plasma case, where the deflection angle is greater than the vacuum case. As shown in Fig. 6, we investigate the effect of the plasma parameters on the deflection angle. Here, the values of the deflection angle increase under the influence of the uniform plasma frequency.

Non-uniform plasma distribution: Here, we consider the non-singular isothermal sphere (SIS). The SIS density distribution can be expressed as follows:

$$\rho(r) = \frac{\sigma_v^2}{2\pi r^2}, \quad (30)$$

where σ_v^2 represents a one-dimensional velocity dispersion. Hence, the analytical expression for the plasma concentration is expressed as follows:



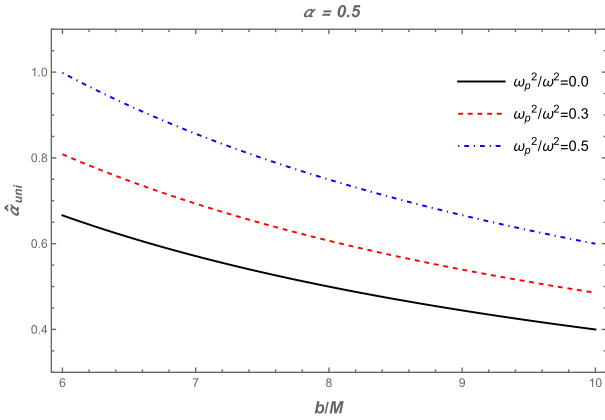


Fig. 6. (color online) Deflection angle $\hat{\alpha}_{uni}$ as a function of the impact parameter b for the different values of the plasma frequency. Here, $\alpha = 0.5$.

$$N(r) = \frac{\rho(r)}{km_p}, \quad (31)$$

where m_p and k represent proton mass and a dimensionless constant, respectively. The plasma frequency can be then expressed as follows:

$$\omega_e^2 = K_e N(r) = \frac{K_e \sigma_v^2}{2\pi k m_p r^2}. \quad (32)$$

To conduct a more detailed analysis of the non-uniform plasma (SIS) effect, it is crucial to derive the explicit expression for the deflection angle around the BH, expressed as follows:

$$\hat{\alpha}_{SIS} = \hat{\alpha}_{SIS1} + \hat{\alpha}_{SIS2} + \hat{\alpha}_{SIS3}. \quad (33)$$

Using Eqs. (24), (28), and (33), we can derive the expression for the deflection angle and introduce the additional plasma constant ω_c^2 in its explicit form

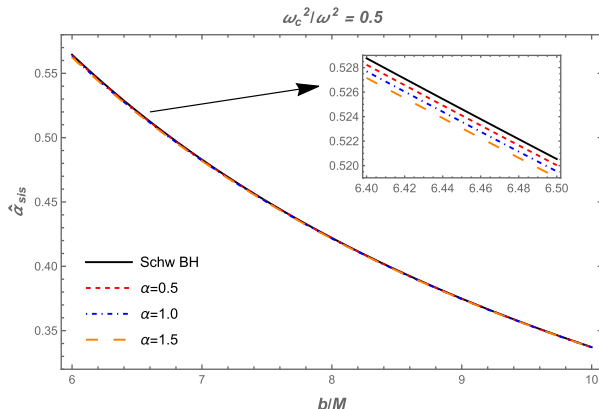


Fig. 7. (color online) Dependence of the deflection angle $\hat{\alpha}_{SIS}$ on the impact parameter b for the different values of the parameter α (left panel) and plasma frequency (right panel).

$$\omega_c^2 = \frac{K_e \sigma_v^2}{2\pi k m_p R_S^2}. \quad (34)$$

where $R_S = 2M$. **Fig. 7** shows the dependence of the deflection angle around the quantum-corrected BH on the impact parameter b for different values of the α parameter and non-uniform plasma frequency. Herein, **Fig. 7** the deflection angle decreases with an increase in the non-uniform plasma frequency. Further, there is a slight decrease in the values of the deflection angle with an increase of the α parameter. The non-uniform plasma has an opposite effect on the deflection angle than the uniform plasma case. For clarity, we have plotted both cases in a single plot, thereby keeping the plasma frequencies constant (see **Fig. 8**).

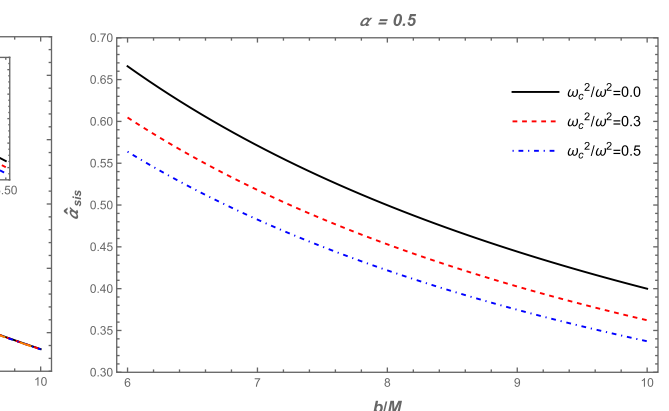
IV. MAGNIFICATION OF GRAVITATIONALLY LENSED IMAGE

In this section, we investigate the magnification of the gravitationally lensed image around the quantum-corrected BH using the deflection angle of the light. Hence, we present the following equation, which combines the light angles $\hat{\alpha}_b$, θ , and β around the black hole [64, 91]:

$$\theta D_s = \beta D_s + \hat{\alpha}_b D_{ds}, \quad (35)$$

where D_d represents the distance between the lens and the observer, D_s the source and observer, D_d the lens and observer, and D_{ds} the source and lens. θ and β represent the angular position of the image and source, respectively. The angular position of the source β can be expressed using Eq. (35) as follows:

$$\beta = \theta - \frac{D_{ds}}{D_s} \frac{\xi(\theta)}{D_d} \frac{1}{\theta}, \quad (36)$$



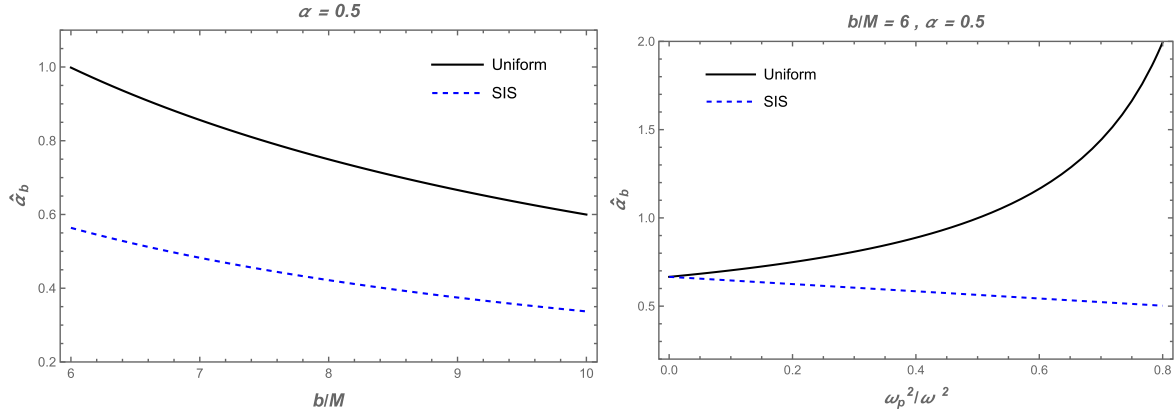


Fig. 8. (color online) Left panel: The dependence of the deflection angle $\hat{\alpha}_b$ on the impact parameter b . Here, α parameter equals to 0.5. Right panel: The deflection angle $\hat{\alpha}_b$ against the plasma parameters. The other parameters are $b/M = 6$ and $\alpha = 0.5$.

with $\xi(\theta) = |\hat{\alpha}_b|b$ and $b = D_d\theta$. The image can be identified as Einstein's ring with a radius of $R_s = D_d\theta_E$, assuming it appears as a ring. In this case, the corresponding angular part θ_E is expressed as

$$\theta_E = \sqrt{2R_s \frac{D_{ds}}{D_d D_s}}. \quad (37)$$

Then the brightness magnification yields

$$\mu_\Sigma = \frac{I_{\text{tot}}}{I_*} = \sum_k \left| \left(\frac{\theta_k}{\beta} \right) \left(\frac{d\theta_k}{d\beta} \right) \right|, \quad k = 1, 2, \dots, j, \quad (38)$$

where I_* and I_{tot} represent the unlensed brightness of the source and total brightness, respectively. The magnification of the source can be expressed as follows [92–95]:

$$\mu_+^{\text{pl}} = \frac{1}{4} \left(\frac{x}{\sqrt{x^2 + 4}} + \frac{\sqrt{x^2 + 4}}{x} + 2 \right), \quad (39)$$

$$\mu_-^{\text{pl}} = \frac{1}{4} \left(\frac{x}{\sqrt{x^2 + 4}} + \frac{\sqrt{x^2 + 4}}{x} - 2 \right). \quad (40)$$

The magnification of the source is then expressed as μ , where $x = \beta/\theta_E$ represents the dimensionless parameter and μ_+^{pl} and μ_-^{pl} the images. Consequently, the total magnification can be written as a linear combination of the images as follows:

$$\mu_{\text{tot}}^{\text{pl}} = \mu_+^{\text{pl}} + \mu_-^{\text{pl}} = \frac{x^2 + 2}{x \sqrt{x^2 + 4}}. \quad (41)$$

In the next, we explore the magnification of the source for two different cases: uniform and non-uniform plasma distributions surrounding the quantum-corrected BH.

Uniform plasma medium case: Herein, we consider

the uniform plasma medium to explore the magnification of the lensed image as aforementioned. Therefore, Eq. (41) can be rewritten for the uniform plasma that surrounds the quantum-corrected BH as follows:

$$\mu_{\text{tot}}^{\text{pl}} = \mu_+^{\text{pl}} + \mu_-^{\text{pl}} = \frac{x_{\text{uni}}^2 + 2}{x_{\text{uni}} \sqrt{x_{\text{uni}}^2 + 4}}, \quad (42)$$

Here, the images $(\mu_+^{\text{pl}})_{\text{uni}}$ and $(\mu_-^{\text{pl}})_{\text{uni}}$ are expressed by

$$(\mu_+^{\text{pl}})_{\text{uni}} = \frac{1}{4} \left(\frac{x_{\text{uni}}}{\sqrt{x_{\text{uni}}^2 + 4}} + \frac{\sqrt{x_{\text{uni}}^2 + 4}}{x_{\text{uni}}} + 2 \right), \quad (43)$$

and

$$(\mu_-^{\text{pl}})_{\text{uni}} = \frac{1}{4} \left(\frac{x_{\text{uni}}}{\sqrt{x_{\text{uni}}^2 + 4}} + \frac{\sqrt{x_{\text{uni}}^2 + 4}}{x_{\text{uni}}} - 2 \right), \quad (44)$$

with

$$x_{\text{uni}} = \frac{\beta}{(\theta_E^{\text{pl}})_{\text{uni}}}. \quad (45)$$

We numerically investigated the total magnification in the uniform plasma case. Fig. 9 shows the dependence of the total magnification of the image $\mu_{\text{tot}}^{\text{pl}}$ on the uniform plasma frequency for different values of the α parameter with a fixed impact parameter of $b = 6M$. As shown in this figure, there is a slight decrease with an increase in the α parameter. Further, the total magnification values increase as the uniform plasma frequency increases.

Non-uniform plasma medium case: We investigate the behavior of the total magnification by considering a non-uniform plasma (SIS). The following equations express the non-uniform plasma case:

$$(\mu_{\text{tot}}^{\text{pl}})_{\text{SIS}} = (\mu_+^{\text{pl}})_{\text{SIS}} + (\mu_-^{\text{pl}})_{\text{SIS}} = \frac{x_{\text{SIS}}^2 + 2}{x_{\text{SIS}} \sqrt{x_{\text{SIS}}^2 + 4}}, \quad (46)$$

with

$$(\mu_{+}^{\text{pl}})_{\text{SIS}} = \frac{1}{4} \left(\frac{x_{\text{SIS}}}{\sqrt{x_{\text{SIS}}^2 + 4}} + \frac{\sqrt{x_{\text{SIS}}^2 + 4}}{x_{\text{SIS}}} + 2 \right), \quad (47)$$

$$(\mu_{-}^{\text{pl}})_{\text{SIS}} = \frac{1}{4} \left(\frac{x_{\text{SIS}}}{\sqrt{x_{\text{SIS}}^2 + 4}} + \frac{\sqrt{x_{\text{SIS}}^2 + 4}}{x_{\text{SIS}}} - 2 \right), \quad (48)$$

where x_{SIS} represents

$$x_{\text{SIS}} = \frac{\beta}{(\theta_E^{\text{pl}})_{\text{SIS}}}.$$

Using Eq. (46), the total magnification can be expressed as a function of the plasma parameter. It can be seen from Fig. 10, the total magnification decreases with an increase in the non-uniform plasma parameter. Moreover, the total magnification of lensed images decreases under the influence of the quantum corrected parameter α acting as a repulsive gravitational charge, which results in the weakening of the gravitational field around the BH. The effect of α is similar to uniform and non-uniform plasma distributions. However, the total magnification decreases in the presence of non-uniform plasma than uniform plasma.

V. CONCLUSION

In this study, we considered a quantum-corrected BH in the Quantum Oppenheimer-Snyder model within the context of loop quantum gravity and investigated its optical properties, thereby revealing notable deviations from GR. First, we explored the motion of photons around a quantum corrected BH surrounded by a plasma medium. Our numerical results showed the relationship between the radius of the photon sphere and plasma frequency, as shown in Fig. 1. We found that the photon sphere radius increases with the plasma parameter, while it decreases with an increase in the quantum correction parameter α . We further investigated the BH shadow under the combined effects of the quantum correction parameter and plasma medium parameter. Using a similar approach to the photon radii, we determined the BH radius and showed that it decreases owing to the combined effects of the plasma and quantum correction parameter, as shown in Fig. 3.

Additionally, we used the obtained results to determine the constraints on the quantum correction parameter, as the shadow size depends on the BH parameters (Fig. 4). Using observational data from M87* and Sgr A*, we determined the possible range of constraints for the quantum correction and plasma parameters. Our findings on the constrained values are valuable and can be potentially applied to M87* and Sgr A* images to provide in-

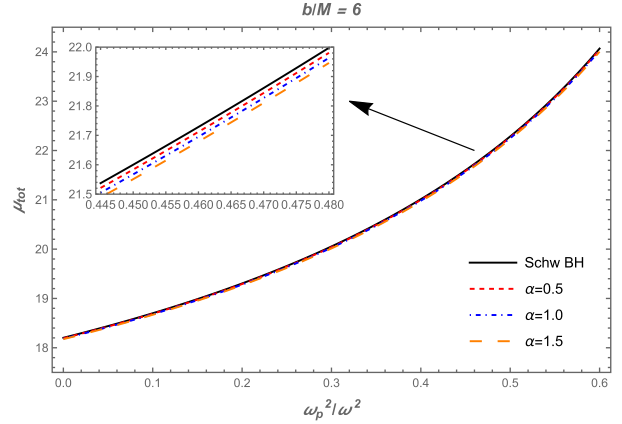


Fig. 9. (color online) Total magnification μ_{tot} as a function of the plasma frequency ω_p^2/ω^2 for different values of the α parameter. Here, $b = 6M$.

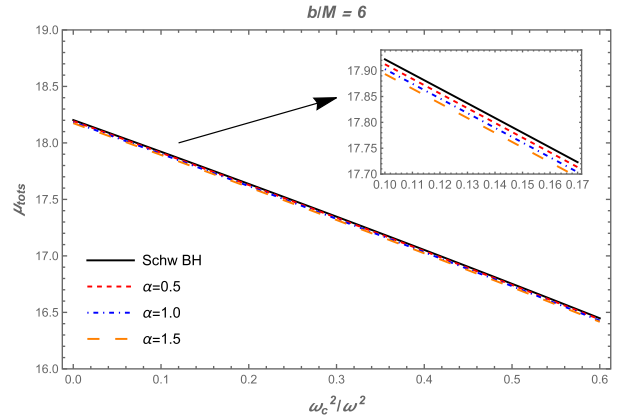


Fig. 10. (color online) Dependence of the total magnification μ_{tot} on the plasma frequency ω_c^2/ω^2 for different values of the α parameter. Here, $b = 6M$.

sights and a constraint range on the quantum correction parameter within astrophysical observations, including data on gravitational lensing effects (see [96–98]).

We further investigated the gravitational lensing in the weak form around a quantum-corrected BH, including the effects of the plasma medium. We considered two independent possible cases: uniform and non-uniform plasma cases. We examined the behavior of the deflection angle resulting from the combined effects of the quantum correction and both uniform and non-uniform plasma parameters. Our results showed that the deflection angle $\hat{\alpha}_{\text{uni}}$ decreases owing to the quantum correction parameter α , while it increases with an increase in the uniform plasma parameter, as shown in Figs. 5 and 6. However, the deflection angle decreases as a function of the impact parameter under the combined effects of quantum correction and uniform plasma parameters. In the non-uniform plasma case, the deflection angle $\hat{\alpha}_{\text{sis}}$ changes at a similar rate owing to the combined effects of the quantum correction and non-uniform plasma parameters, thereby resulting in the deflection angle shifting

downward and decreasing to possibly smaller values (Fig. 7). Notably, the light traveling through the uniform plasma medium can be strongly deflected than the non-uniform plasma, thereby leading to a significant difference in the deflection angle for uniform and non-uniform plasma distributions (Fig. 8).

Finally, we explored the variation in the total magnification, $\mu_{\text{tot}}^{\text{pl}}$, of the lensed image under the effect of the quantum correction parameter α , including the effects of uniform and non-uniform plasma distributions, as shown in Figs. 9 and 10. Our findings show that the total magnification curves shift downward to smaller values owing to the impact of the quantum correction parameter α , which is similar to the observed behavior of the deflection angle, while it increases/decreases significantly by the

uniform/non-uniform plasma effects.

The results showed that the quantum correction parameter, α , can alter the null geodesics, thereby resulting in a decrease in the radii of the photon sphere and BH shadow. This behavior corresponds with the physical interpretation of the quantum correction parameter as a repulsive gravitational charge, which weakens the gravitational field strength near the quantum-corrected BH. This effect, although small, remains significant in astrophysical contexts, particularly when considered alongside the effects of the plasma medium. Our findings provide insights into the quantum-corrected BHs and contribute to evaluating and constraining the validity of alternative models to BHs in GR and loop quantum gravity, particularly when making astrophysical observations and predictions.

References

- [1] S. W. Hawking and G. F. R. Ellis, *The large-scale structure of space-time* (Cambridge: Cambridge University Press, 1973)
- [2] A. Borde, A. H. Guth, and A. Vilenkin, *Phys. Rev. Lett.* **90**, 151301 (2003), arXiv: gr-qc/0110012[gr-qc]
- [3] A. Borde and A. Vilenkin, *Phys. Rev. Lett.* **72**, 3305 (1994), arXiv: gr-qc/9312022[gr-qc]
- [4] R. J. Adler, *Am. J. Phys.* **78**, 925 (2010), arXiv: 1001.1205[gr-qc]
- [5] Y. J. Ng, *Mod. Phys. Lett. A* **18**, 1073 (2003), arXiv: grqc/0305019[gr-qc]
- [6] B. P. Abbott and *et al.* (Virgo and LIGO Scientific Collaborations), *Phys. Rev. Lett.* **116**, 061102 (2016), arXiv: 1602.03837[gr-qc]
- [7] B. P. Abbott and *et al.* (Virgo and LIGO Scientific Collaborations), *Phys. Rev. Lett.* **116**, 241102 (2016), arXiv: 1602.03840[gr-qc]
- [8] K. Akiyama and *et al.* (Event Horizon Telescope Collaboration), *Astrophys. J.* **875**, L1 (2019), arXiv: 1906.11238[astro-ph.GA]
- [9] K. Akiyama and *et al.* (Event Horizon Telescope Collaboration), *Astrophys. J.* **875**, L6 (2019), arXiv: 1906.11243[astro-ph.GA]
- [10] A. Ashtekar and J. Lewandowski, *Class. Quantum Gravity* **21**, R53 (2004), arXiv: gr-qc/0404018[gr-qc]
- [11] P. Singh and A. Toporensky, *Phys. Rev. D* **69**, 104008 (2004), arXiv: gr-qc/0312110[gr-qc]
- [12] A. Ashtekar, T. Pawłowski, and P. Singh, *Phys. Rev. D* **74**, 084003 (2006), arXiv: gr-qc/0607039[gr-qc]
- [13] A. Ashtekar, T. Pawłowski, and P. Singh, *Phys. Rev. Lett.* **96**, 141301 (2006), arXiv: gr-qc/0602086[gr-qc]
- [14] G. Date and G. M. Hossain, *Phys. Rev. Lett.* **94**, 011302 (2005), arXiv: gr-qc/0407074[gr-qc]
- [15] A. Ashtekar and P. Singh, *Class. Quantum Gravity* **28**, 213001 (2011), arXiv: 1108.0893[gr-qc]
- [16] T. Papanikolaou, *Class. Quantum Gravity* **40**, 134001 (2023), arXiv: 2301.11439[gr-qc]
- [17] B.-F. Li and P. Singh, arXiv: 2304.05426 [gr-qc]
- [18] L. Modesto, *Int. J. Theor. Phys.* **49**, 1649 (2010), arXiv: 0811.2196[gr-qc]
- [19] L. Modesto and I. Prémont-Schwarz, *Phys. Rev. D* **80**, 064041 (2009), arXiv: 0905.3170[hep-th]
- [20] S. Sahu, K. Lochan, and D. Narasimha, *Phys. Rev. D* **91**, 063001 (2015), arXiv: 1502.05619[gr-qc]
- [21] A. Ashtekar, J. Olmedo, and P. Singh, *Phys. Rev. Lett.* **121**, 241301 (2018), arXiv: 1806.00648[gr-qc]
- [22] A. Ashtekar, J. Olmedo, and P. Singh, *Phys. Rev. D* **98**, 126003 (2018), arXiv: 1806.02406[gr-qc]
- [23] M. Bojowald, S. Brahma, and D.-H. Yeom, *Phys. Rev. D* **98**, 046015 (2018), arXiv: 1803.01119[gr-qc]
- [24] E. Alesci, S. Bahrami, and D. Pranzetti, *Phys. Lett. B* **797**, 134908 (2019), arXiv: 1904.12412[gr-qc]
- [25] M. Assanioussi, A. Dapor, and K. Liegener, *Phys. Rev. D* **101**, 026002 (2020), arXiv: 1908.05756[gr-qc]
- [26] N. Bodendorfer, F. M. Mele, and J. Münch, *Phys. Lett. B* **819**, 136390 (2021), arXiv: 1911.12646[gr-qc]
- [27] A. Ashtekar, *Universe* **6**, 21 (2020), arXiv: 2001.08833[grqc]
- [28] W.-C. Gan, N. O. Santos, F.-W. Shu *et al.*, *Phys. Rev. D* **102**, 124030 (2020), arXiv: 2008.09664[grqc]
- [29] A. Perez, *Rep. Prog. Phys.* **80**, 126901 (2017), arXiv: 1703.09149[gr-qc]
- [30] Y.-C. Liu, J.-X. Feng, F.-W. Shu *et al.*, *Phys. Rev. D* **104**, 106001 (2021), arXiv: 2109.02861[gr-qc]
- [31] Q.-M. Fu and X. Zhang, *Phys. Rev. D* **105**, 064020 (2022), arXiv: 2111.07223[gr-qc]
- [32] S. Brahma, C.-Y. Chen, and D.-H. Yeom, *Phys. Rev. Lett.* **126**, 181301 (2021), arXiv: 2012.08785[gr-qc]
- [33] S. Yang, W.-D. Guo, Q. Tan *et al.*, *Phys. Rev. D* **108**, 024055 (2023), arXiv: 2304.06895[gr-qc]
- [34] J.-M. Yan, C. Liu, T. Zhu *et al.*, *Phys. Rev. D* **107**, 084043 (2023), arXiv: 2302.10482[gr-qc]
- [35] S. Albuquerque, I. P. Lobo, and V. B. Bezerra, *Class. Quant. Grav.* **40**, 174001 (2023), arXiv: 2301.07746[grqc]
- [36] H. X. Jiang, C. Liu, I. K. Dihingia *et al.*, *JCAP* **01**, 059 (2024), arXiv: 2312.04288[gr-qc]
- [37] H. Jiang, M. Alloqulov, Q. Wu *et al.*, *Phys. Dark Universe* **46**, 101627 (2024)
- [38] J. Synge, *Mon. Not. R. Astron. Soc.* **131**, 463 (1966)
- [39] J. Luminet, *Astron. Astrophys.* **75**, 228 (1979)
- [40] L. Amarilla and E. F. Eiroa, *Phys. Rev. D* **87**, 044057 (2013), arXiv: 1301.0532[gr-qc]
- [41] S.-W. Wei and Y.-X. Liu, *J. Cosmol. Astropart. Phys.* **11**, 063 (2013), arXiv: 1311.4251[gr-qc]
- [42] R. A. Konoplya, *Phys. Lett. B* **795**, 1 (2019), arXiv: 1905.00064[gr-qc]
- [43] S. Vagnozzi and L. Visinelli, *Phys. Rev. D* **100**, 024020 (2019)

- [44] M. Afrin, R. Kumar, and S. G. Ghosh, *Mon. Not. R. Astron. Soc.* **504**, 5927 (2021), arXiv: 2103.11417[gr-qc]
- [45] F. Atamurotov, S. G. Ghosh, and B. Ahmedov, *Eur. Phys. J. C* **76**, 273 (2016), arXiv: 1506.03690[gr-qc]
- [46] R. A. Konoplya and A. Zhidenko, *Phys. Rev. D* **100**, 044015 (2019)
- [47] G. Mustafa, F. Atamurotov, I. Hussain *et al.*, *Chin. Phys. C* **46**, 125107 (2022), arXiv: 2207.07608[gr-qc]
- [48] N. Tsukamoto, Z. Li, and C. Bambi, *J. Cosmol. Astropart. Phys.* **2014**, 043 (2014)
- [49] F. Atamurotov, S. Shaymatov, P. Sheoran *et al.*, *J. Cosmol. Astropart. Phys.* **2021**, 045 (2021), arXiv: 2105.02214[gr-qc]
- [50] N. Tsukamoto, *Phys. Rev. D* **97**, 064021 (2018)
- [51] J. L. Rosa, *Phys. Rev. D* **107**, 084048 (2023)
- [52] J. Badía and E. F. Eiroa, *Phys. Rev. D* **107**, 124028 (2023), arXiv: 2210.03081[gr-qc]
- [53] A. Al-Badawi, M. Alloqulov, S. Shaymatov *et al.*, *Chin. Phys. C* **48**, 095105 (2024), arXiv: 2401.04584[gr-qc]
- [54] G. J. Olmo, J. L. Rosa, D. Rubiera-Garcia *et al.*, *Class. Quantum Gravity* **40**, 174002 (2023)
- [55] R. A. Konoplya and A. Zhidenko, *Phys. Rev. D* **103**, 104033 (2021)
- [56] S. H. Hindi, K. Jafarzade, and B. Eslam Panah, *J. Cosmol. Astropart. Phys.* **2023**, 022 (2023), arXiv: 2206.05132[gr-qc]
- [57] J. W. Moffat, *Eur. Phys. J. C* **75**, 130 (2015), arXiv: 1502.01677[gr-qc]
- [58] J. W. Moffat and V. T. Toth, *Phys. Rev. D* **101**, 024014 (2020), arXiv: 1904.04142[gr-qc]
- [59] A. Al-Badawi, S. Shaymatov, M. Alloqulov *et al.*, *Commun. Theor. Phys.* **76**, 085401 (2024), arXiv: 2401.12723[gr-qc]
- [60] A. S. Eddington, *The Observatory* **42**, 119 (1919)
- [61] G. S. Bisnovatyi-Kogan and O. Y. Tsupko, *Mon. Not. R. Astron. Soc.* **404**, 1790 (2010)
- [62] O. Y. Tsupko and G. S. Bisnovatyi-Kogan, *Gravit. Cosmol.* **18**, 117 (2012)
- [63] P. V. P. Cunha, N. A. Eiró, C. A. R. Herdeiro *et al.*, *J. Cosmol. A. P* **2020**, 035 (2020), arXiv: 1912.08833[gr-qc]
- [64] G. Z. Babar, F. Atamurotov, and A. Z. Babar, *Phys. Dark Universe* **32**, 100798 (2021)
- [65] W. Javed, M. Atique, and A. Övgün, *Gen. Relativ. Gravit.* **54**, 135 (2022), arXiv: 2210.17277[gr-qc]
- [66] K. Jafarzade, M. Kord Zangeneh, and F. S. N. Lobo, *J. Cosmol. Astropart. Phys.* **2021**, 008 (2021), arXiv: 2010.05755[gr-qc]
- [67] F. Atamurotov, D. Ortiqboev, A. Abdujabbarov, and G. Mustafa, *Eur. Phys. J. C* **82**, 659 (2022)
- [68] A. Övgün, İ. Sakalli, and J. Saavedra, *Ann. Phys.* **411**, 167978 (2019), arXiv: 1806.06453[gr-qc]
- [69] S. Rahvar and J. W. Moffat, *MNRAS* **482**, 4514 (2019), arXiv: 1807.07424[gr-qc]
- [70] R. N. Izmailov, R. K. Karimov, E. R. Zhdanov *et al.*, *MNRAS* **483**, 3754 (2019), arXiv: 1905.01900[gr-qc]
- [71] A. Al-Badawi, S. Shaymatov, S. K. Jha *et al.*, *Eur. Phys. J. C* **84**, 722 (2024), arXiv: 2406.17501[gr-qc]
- [72] A. Al-Badawi, S. Shaymatov, and İ. Sakalli, *Eur. Phys. J. C* **84**, 825 (2024), arXiv: 2408.09228[gr-qc]
- [73] A. Rogers, *Mon. Not. R. Astron. Soc.* **451**, 17 (2015)
- [74] G. Z. Babar, A. Z. Babar, and F. Atamurotov, *Eur. Phys. J. C* **80**, 761 (2020)
- [75] W. Javed, S. Riaz, R. C. Pantig *et al.*, *Eur. Phys. J. C* **82**, 1057 (2022), arXiv: 2212.00804[gr-qc]
- [76] W. Javed, I. Hussain, and A. Övgün, *Eur. Phys. J. Plus* **137**, 148 (2022), arXiv: 2201.09879[gr-qc]
- [77] C. Benavides-Gallego, A. Abdujabbarov, and C. Bambi, *Eur. Phys. J. C* **78**, 694 (2018)
- [78] F. Atamurotov, S. Shaymatov, and B. Ahmedov, *Galaxies* **9**, 54 (2021)
- [79] F. Atamurotov, M. Alloqulov, A. Abdujabbarov *et al.*, *Eur. Phys. J. Plus* **137**, 634 (2022)
- [80] J. Lewandowski, Y. Ma, J. Yang *et al.*, *Phys. Rev. Lett.* **130**, 101501 (2023)
- [81] J.-P. Ye, Z.-Q. He, A.-X. Zhou *et al.*, *Phys. Lett. B* **851**, 138566 (2024), arXiv: 2312.17724[gr-qc]
- [82] C.-Y. Shao, C. Zhang, W. Zhang *et al.*, *Phys. Rev. D* **109**, 064012 (2024), arXiv: 2309.04962[gr-qc]
- [83] C. Zhang, Y. Ma, and J. Yang, *Phys. Rev. D* **108**, 104004 (2023), arXiv: 2302.02800[gr-qc]
- [84] H. Gong, S. Li, D. Zhang, G. Fu *et al.*, *Phys. Rev. D* **110**, 044040 (2024), arXiv: 2312.17639[gr-qc]
- [85] S. Yang, Y.-P. Zhang, T. Zhu *et al.*, arXiv: 2407.00283
- [86] J. L. Synge, *Relativity: The General Theory* (Amsterdam: North-Holland Pub. Co., 1960)
- [87] O. Y. Tsupko and G. S. Bisnovatyi-Kogan, *Gravit. Cosmol.* **15**, 184 (2009)
- [88] V. Perlick, O. Y. Tsupko, and G. S. Bisnovatyi-Kogan, *Phys. Rev. D* **92**, 104031 (2015), arXiv: 1507.04217[grqc]
- [89] K. Akiyama and *et al.* (Event Horizon Telescope Collaboration), *Astrophys. J.* **910**, L12 (2021)
- [90] C. Bambi, K. Freese, S. Vagnozzi *et al.*, *Phys. Rev. D* **100**, 044057 (2019)
- [91] V. Bozza, *Phys. Rev. D* **78**, 103005 (2008)
- [92] F. Atamurotov, A. Abdujabbarov, and J. Rayimbaev, *Eur. Phys. J. C* **81**, 118 (2021)
- [93] M. Alloqulov, F. Atamurotov, A. Abdujabbarov *et al.*, *Chin. Phys. C* **47**, 075103 (2023)
- [94] M. Alloqulov, F. Atamurotov, A. Abdujabbarov *et al.*, *Chin. Phys. C* **48**, 025104 (2024)
- [95] M. Alloqulov, S. Shaymatov, A. Jawad *et al.*, *Commun. Theor. Phys.* **77**, 015402 (2025)
- [96] Y. Wang, *J. Cosmol. Astropart. Phys.* **2005**, 005 (2005), arXiv: astro-ph/0406635[astro-ph]
- [97] E. J. Gonzalez, G. Foëx, J. L. Nilo Castellón *et al.*, *MNRAS* **452**, 2225 (2015), arXiv: 1504.03364[astro-ph.CO]
- [98] Z. Kalantari, S. Rahvar, and A. Ibrahim, *Astrophys. J.* **934**, 106 (2022), arXiv: 2205.05278[astroph.HE]